

MRS Advances © 2017 Materials Research Society  
DOI: 10.1557/adv.2017.122

## Effect of annealing and process parameters on microstructure and properties of DC Magnetron Sputtered Ni-Zr alloy thin films

Bibhu P. Sahu, Rahul Mitra

Department of Metallurgical and Materials Engineering, Indian Institute of Technology, Kharagpur, 721302, West Bengal, India

### ABSTRACT

Ni-Zr alloy thin films were processed by DC magnetron sputtering of high purity Ni and Zr targets in ultrahigh vacuum at ambient temperature, with the substrate being subjected to either 0 V or -60 V bias. Some of the as-deposited films were annealed in vacuum at 700°C for 1 h. Surface profilometer and atomic force microscope were used to measure the film thickness and surface roughness, respectively. X-ray diffraction and cross-sectional TEM analysis have shown dispersion of nano-sized Ni<sub>3</sub>Zr dispersed in nanocrystalline Ni matrix. Nano-indentation and scratch tests conducted at 2 mN load have shown variation of hardness, Young's modulus, scratch resistance, and coefficient of friction with substrate bias and annealing due to changes in grain size and surface roughness.

### INTRODUCTION

Thin films of Ni-Zr alloy have been found to be attractive because of the possibility of their growth with both crystalline and amorphous structure depending on the composition. A recent study by Turnow and co-workers [1] has shown that the binary Ni-Zr alloy thin films prepared by dc magnetron sputtering possess amorphous structure for compositions having 16-93 at. % Ni. Magnetron co-sputtering of multiple targets for deposition of alloy thin films has now become most convenient way of processing, because it allows a wide range of compositions to form. Here, the desirable purity of the films is easily achieved by use of high purity targets and Ar gas for sputtering. The Ni-Zr alloy films have been investigated for application in fuel cells, biomedical industries, stressed atomic force microscopy probes, and most importantly in nuclear reactor engineering, as well as for hydrogen storage and separation [2]. The amorphous Ni-Zr alloy films have been found to undergo crystallization on annealing at temperatures in the range of 650-750°C [3]. Crystallization of these films leads to the formation of Ni-Zr based binary intermetallic phases like Ni<sub>3</sub>Zr, which possess higher hardness, as well as greater resistance to both wear and corrosion compared to that of pure Ni, and therefore could be used as nanocomposite protective coatings [4, 5]. Furthermore, nanocrystallinity of the Ni-Zr alloy films is preferred for better hydrogen-sorption properties, and use for hydrogen storage [6].

The scope of the present study includes processing of nanocrystalline Ni-Zr alloy films by dc magnetron co-sputtering of high purity Ni and Zr targets with or without substrate bias, annealing of the as-deposited films at 700°C, study of microstructure using scanning and transmission electron microscopy, as well as evaluation of surface roughness, nanoindentation hardness, Young's modulus, and scratch resistance.

## EXPERIMENTAL DETAILS

The films were deposited on p-type Si (100) substrates by DC magnetron sputtering system (model KVS-T 4065, Korea Vacuum Tech., Gyeonggi-do, South Korea) using high purity targets of Ni and Zr (99.99 % purity) in argon atmosphere (purity 99.9998 %). The process parameters used for the depositions are shown in the Table I. The silicon wafers were ultrasonically cleaned first with acetone and then using ethyl alcohol. Further, some of the films deposited without application of substrate bias were annealed in vacuum at 700°C for 1 h, and their microstructures and mechanical properties were compared with those of the as-deposited films.

The films were characterized by grazing incidence X-ray diffraction (GIXRD) using Cu K $\alpha$  radiation within the 2 $\theta$  range of 30<sup>0</sup>-65<sup>0</sup>, keeping the angle of 1.5<sup>0</sup> between the detector and specimen plane. The thicknesses of the films were measured by using a surface profilometer (Dektak 150) equipped with a diamond tip stylus at a load of 30  $\mu$ N. The microstructure in cross-sectional view were observed using transmission electron microscope (TEM), whereas the chemical compositions were assessed by energy dispersive X-ray spectroscopy (EDS). Mechanical properties were evaluated by nanoindentation hardness using a nanoindenter having a Berkovich indenter with tip radius of  $\approx$ 50 nm, which was operated at a loading rate of 0.2 mN/s to a maximum load of 2 mN. Further using same load and indenter, nano-scratch tests were carried out with a lateral speed of 0.5  $\mu$ m/s to a length of  $\approx$ 20  $\mu$ m. Surface roughness of the as-deposited and annealed films were observed using atomic force microscopy.

**Table I. Process parameters used for the depositions**

Process parameters	Values
Base pressure	2.0 X 10 <sup>-6</sup> Torr
Working pressure	20 mTorr
Ni DC power	200 Watt
Zr DC power	100Watt
Deposition temperature	Room temperature
Substrate bias voltage	0, -60 V
Time of deposition	15 minutes
Substrate rotation	20 RPM
Target to substrate distance	120 mm

## RESULTS AND DISCUSSION

### Microstructure and Phase analysis

The average bulk composition of the as-deposited films, as found by EDX analysis on TEM is Ni<sub>80</sub>Zr<sub>20</sub>. Figure 1 shows the GIXRD patterns of the Ni<sub>80</sub>Zr<sub>20</sub> films deposited under

various conditions. All the patterns indicate the presence of FCC Ni (PDF No. 00-004-0850) and hexagonal Ni<sub>3</sub>Zr phase (PDF No. 00-029-0946), which is generally formed in the composition range of 22-28 atom % Zr, as predicted by the Ni-Zr binary phase diagram [7]. However, in the GIXRD pattern from the film annealed after growth using 0 V substrate bias, a peak representing the monoclinic ZrO<sub>2</sub> phase (PDF No. 01-078-0047) is detected at  $2\theta=58.4^\circ$  in addition to the peaks of Ni and Ni<sub>3</sub>Zr phases. Crystallite sizes obtained by analyzing the GIXRD results using both Williamson-Hall relation and Scherrer equation as well as measurement from dark field TEM images are shown in Table II. Comparison of the grain size values calculated by using XRD-based methods and several dark field TEM images shows excellent agreement. These results further indicate that the average grain size is finer in the film grown with substrate bias of -60 V compared to that in the film grown without bias. These results are consistent with the peaks in the GIXRD pattern from the film grown using -60 V substrate bias being wider than those in the film grown without substrate bias (Figure 1).

In contrast to the observations related to the as-deposited film, relatively sharper peaks are found in the GIXRD pattern representing the annealed film, which is consistent with coarser grain size mentioned in Table II. Further, the peaks for Ni<sub>3</sub>Zr at positions 1 and 2 in the XRD pattern from the film grown using -60 V substrate bias are found to shift to lower  $2\theta$  value with respect to their positions for the film grown without bias. As Zr has higher atomic radius compared to that of Ni, the lattice constant of substitutional solid solution of Ni (Zr) is expected to increase with increasing Zr concentration. Therefore, the change in XRD peak position with respect to that of pure Ni is attributed to higher amount of Zr in solid solution in Ni matrix in the film grown using -60 V substrate bias. As shown in Table II, the volume fraction of Ni<sub>3</sub>Zr precipitate calculated from Rietveld analysis is found to decrease from 16 % in the film grown without bias to 12 % in those grown using -60 V substrate bias, which is suggestive of a higher amount of Zr in solid solution in the former film. The finer average grain size in the film grown using substrate bias of -60 V as compared to that found on deposition without bias may be attributed to higher density and more uniform distribution of nucleating islands caused through resputtering by Ar<sup>+</sup> ions of the plasma during growth of the former film [8]. Moreover, a higher amount of Zr in the Ni(Zr) solid solution comprising the matrix of the film grown using -60 V substrate bias compared to that in the film grown without bias is also expected to have contributed to finer grain size in the former film.

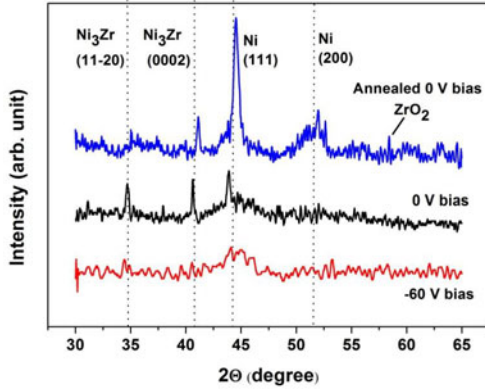


**Figure 1.** GIXRD patterns from various Ni-Zr alloy films.

Examination of bright field cross-section TEM images along with SAED patterns in Figure 2(a) through (f) shows the formation of nanometric grains of Ni and Ni<sub>3</sub>Zr. Presence of thicker rings in the SAED pattern from the film grown using -60 V substrate bias (Fig. 2(e)) compared to those in the pattern from the film grown without substrate bias (Fig. 2(d)) is consistent with the presence of wider peaks in the GIXRD pattern from the former type of film. Comparison of the bright field TEM images shown in Fig. 2(a) and (c) shows that intercolumnar porosities in the film grown without bias, whereas those are not found in the annealed film. However, annealing also caused a limited amount of grain growth as confirmed by the results shown in Table II, and hence the corresponding SAED pattern (Figure 2(f)) consists of spots arranged in the form of distinct rings. Furthermore, the results in Table II indicate that volume fraction of Ni<sub>3</sub>Zr in the annealed film is marginally higher than that in the as-deposited film. The grain growth during annealing is probably restricted by the presence of a uniform distribution of nano-size Ni<sub>3</sub>Zr precipitates, and also by stabilizing effect of a small amount of Zr in solid solution. The retention of small amount of Zr in solid solution on annealing is evident from the XRD peak shift of Ni of  $2\theta=0.02^\circ$  from standard value ICDD data (PDF No. 00-004-0850).

### **Thickness and Surface roughness**

The average thickness values measured using the surface profilometer and surface roughness estimated using AFM are shown in Table II. The results in this table show that films deposited using substrate bias = -60 V have less thickness and roughness compared to that of the film grown without bias, which can be attributed to higher density and more uniform growth, respectively of the former film. Resputtering of the film by Ar<sup>+</sup> ions caused by the application of negative substrate bias enhances the adatom mobility, which in turn leads to both closure of pores through re-arrangement of adatoms as well as more uniform growth of the film [9]. In contrast, the average thickness and surface roughness of the

annealed films are found to be higher than those of the as-deposited films, which may be attributed to grain growth in the former films.

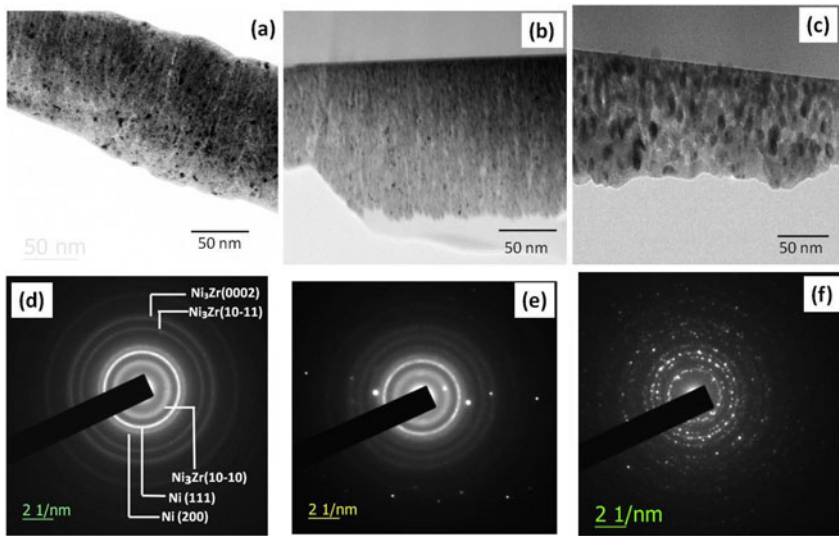


**Figure 2.** Pairs of TEM bright field images and SAED patterns representing the as-deposited  $\text{Ni}_{80}\text{Zr}_{20}$  film grown (a and d) without substrate bias, (b and e) using substrate bias = -60 V, as well as (c) and (f) films grown without substrate bias and then in vacuum at 700°C.

**Table II.** Thickness, grain size, surface roughness, Young's modulus, and hardness of the  $\text{Ni}_{80}\text{Zr}_{20}$  alloy films.

Films	Thickness (nm)	Grain size (nm)		Vol. fr. of $\text{Ni}_3\text{Zr}$ (%)	Surface roughness (nm)	Young's modulus (GPa)	Hardness (GPa)
		Ni (nm)	$\text{Ni}_3\text{Zr}$ (nm)				
0 V	462 ± 10	*9.3 ± 1.1 (WH) *10.2 ± 0.5 (Sch.) *10.5 ± 1.5 (DFTEM)	*6.4 ± 0.9 (WH) *6.2 ± 0.5 (Sch.) *7 ± 1.8 (DFTEM)	16	2.9 ± 0.3	155.3 ± 6.3	5.90 ± 0.12

-60 V	427 ±21	*7.2±0.5 (WH) *6.9±0.5 (Sch.) *7±0.6 (DFTEM)	*5.3±0.2 (WH) * 4.6±0.8 (Sch.) *6±0.4 (DFTEM)	12	2.7 ± 0.2	157.5 ±12.5	7.11 ± 0.18
Annealed	500 ±16	*16.6±1.2 (WH) *17.9±0.5 (Sch.) *19±0.6 (DFTEM)	*18.7±1 (WH) *19.2±0.5 (Sch.) *21±1.3 (DFTEM)	17	4.1 ± 0.6	160 ± 8.5	6.36 ±0.62

- **N.B.** WH- Williamson-Hall relation  
Sch- Scherrer equation  
DFTEM- Dark field TEM images

### **Mechanical properties**

The plots of load against indentation depth obtained from the nano-indentation tests are shown in Figure 3, hardness and Young's modulus are shown in Table II. Examination of the results in this table indicates that the film grown with substrate bias of -60 V has maximum hardness of 7.11 GPa. This observation is recorded in spite of decrease in volume fraction of the Ni<sub>3</sub>Zr precipitates from ≈16% in the film grown without bias to ≈12% in that grown with -60 V bias. Hence by applying negative bias voltage, Zr atoms form substitutional solid solution in the matrix thereby suppressing the formation of Ni<sub>3</sub>Zr precipitate. Higher value of hardness of the nanocomposite film grown at -60 V compared to that of 0 V bias film can be attributed to increased solid solution strengthening of the Ni matrix of the former film. Furthermore, an increase of hardness by ≈7.8% and Young's modulus by ≈3% is observed on annealing of the film grown without bias, which may be attributed to increase in density and marginal increase in volume fraction of Ni<sub>3</sub>Zr precipitates.

Plots depicting the variation of coefficient of friction (COF) with normal load of Ni<sub>80</sub>Zr<sub>20</sub> films as depicted in Figure 4 indicate correlation of this parameter with surface roughness of the films, which in turn influence the nature of its interaction with the nanoindenter tip. The COF values are not only higher for the annealed film, but also show sharp fluctuation with increase in load, which may be attributed to its relatively higher surface roughness. As the interaction between the nanoindenter tip and the film surface is of adhesive character, the COF is found to be directly related to surface roughness. Among the as-deposited films grown with substrate bias of 0 V and -60 V, lower value of COF is observed for the latter film because of its higher hardness, which implies that the depth of penetration of the indenter-tip is less and so is the area of its contact with the surface of the investigated film [9].

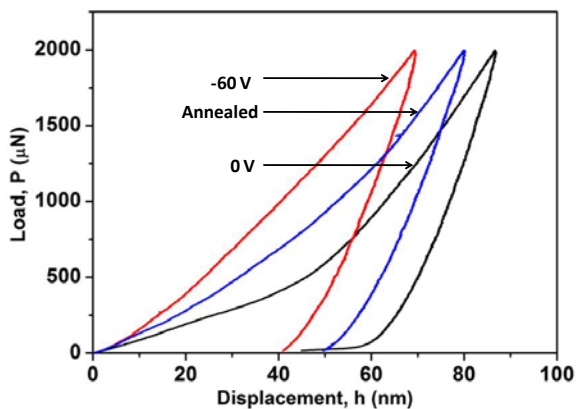


**Figure 3.**Plots depicting load against indentation depth of various films.

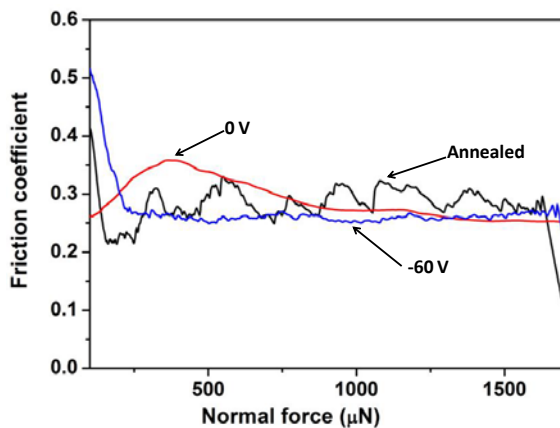


**Figure 4.**Plots depicting the variation of coefficient of friction with normal load of the films.

## CONCLUSIONS

The major conclusions drawn from the present study are as follows:

- Co-sputtering of Ni and Zr targets using powers of 200 and 100 W, respectively leads to the formation of nanocomposite thin films having  $N_3Zr$  dispersed in Ni matrix, with nano-scale grain-size in both the phases.
- Applying bias voltage helps in densification and compaction of the film as well as reduction in the grain size. Higher nanoindentation-hardness of the film grown using -60 V substrate bias as compared to those of the films grown without bias may be attributed

to increased solid solution strengthening of the former type of film, besides marginal reduction in the average grain size as well as increase in density.

- Surface roughness of the film deposited with substrate bias has been found to be less than those of the films deposited without substrate bias or subjected to annealing. This may be attributed to more uniform growth of the film due to higher adatom mobility caused by application of substrate bias.
- Friction coefficient measured using nano-scratch tests is found to be related to both surface roughness and hardness of the films, which in turn affect the amount of interaction of nanoindenter tip with the film surface.

## ACKNOWLEDGEMENTS

The authors would like to thank Mr. Pradip Guha at the Department of Metallurgical and Materials Engineering, as well as Mr. Srikrishna Maity, Mr. Tapas Paul and Mr. Rajiv Kundu of the Central Research Facility for the technical assistance with various types of characterization work.

## REFERENCES

1. H. Turnow, H. Wendrock and S. Menzel, *Thin Solid Films* **561**, 48 (2014).
2. D. Bhattacharya, T.V. Chandrasekhar Rao, K.G. Bhushan and A. Arya, *J. Alloys Compd.* **649**,746 (2015).
3. M. Apreutesei, C. Boissy, N. Mary, P. Steyer, *Acta Materialia* **89**, 305 (2015).
4. M. Ghidelli, S. Gravier and J. Blandin, *J. Alloys Compd.* **615**, 348 (2014).
5. D. P. Wang and S.L. Wang, *Corros.Sci.* **59**, 88 (2012).
6. L. Mihailov, T. Spassov and M. Bojinov, *Int. J. Hydrogen Energy* **37**, 10499 (2012).
7. G. Ghosh, *J.Mater. Res.* **9**, 598 (1994).
8. K.L. Chopra, *Thin Film Phenomena*. (Mc-Graw Hill Book Company, New York, 1969) p. 137.
9. M. Kumar, S.Mishra, R. Mitra, *Surf. Coat.Technol.* 228, 100 (2013); **251**, 239 (2014).